BMJ Open Ophthalmology

Comparison of human amniotic membrane decellularisation approaches for hESC-derived RPE cells culture

Elena Daniele ,[1,2] Barbara Ferrari,[2] Nicolò Rassu,[3] Joshua Ben-Nun,[4] Lorenzo Bosio,[2] Vanessa Barbaro,[2] Stefano Ferrari ,[2] Diego Ponzin[2]

To cite: Daniele E, Ferrari B, Rassu N, *et al*. Comparison of human amniotic membrane decellularisation approaches for hESC-derived RPE cells culture. *BMJ Open Ophthalmology* 2022;**7**:e000981. doi:10.1136/bmjophth-2022-000981

► Additional supplemental material is published online only. To view, please visit the journal online (http://dx.doi.org/10.1136/bmjophth-2022-000981).

ED and BF contributed equally.

Received 20 January 2022
Accepted 24 August 2022

[1]Department of Translational Medicine, University of Ferrara, Ferrara, Italy
[2]Venice Eye Bank, Venice, Italy
[3]Ophthalmic Unit, Ospedale dell'Angelo, Venice, Italy
[4]Medicel AG, CH-9423 Altenrhein, Switzerland

Correspondence to
Dr Elena Daniele; elena.daniele@fbov.it

ABSTRACT

Objective Recent clinical studies have shown that the transplantation of functional retinal pigment epithelium (RPE) cells can prevent the onset of RPE degeneration in age-related macular degeneration. This study aimed to investigate the potential of human amniotic membrane (hAM) as a viable scaffold for the growth and proliferation of pluripotent-derived RPE cells.

Methods and analysis Three enzymatic hAM de-epithelialisation methods (thermolysin, trypsin-EDTA and dispase II) were assessed by histological analysis and optical coherence tomography (OCT). We generated RPE cells from a human embryonic stem cell (hESC) line subjected to spontaneous differentiation in feeder-free conditions. The hESC-derived RPE cells were seeded over denuded hAM at a density of 2.0×10^5 cells/cm^2 and maintained in culture for up to 4 weeks. Immnofluorescence was carried out to evaluate the development of a confluent monolayer of RPE cells on the top of the hAM. Conditioned medium was collected to measure pigment epithelium-derived factor (PEDF) concentration by ELISA.

Results Laminin α5 and collagen IV staining confirmed the efficiency of the de-epithelialisation process. In particular, thermolysin showed good retention of tissue integrity on OCT images and greater preservation of the hAM basement membrane. The hESC-derived RPE cells formed patches of pigmented cells interspersed along the denuded hAM, but failed to form a regular sheet of RPE cells. These cells expressed typical RPE markers, such as PMEL17 and RPE65, but they secreted low levels of PEDF.

Conclusion The biological variability of the hAM could influence the adhesion and the expansion of hESC-derived RPE cells. Further studies are required to verify whether a non-confluent monolayer might represent a limit to transplantation.

WHAT IS ALREADY KNOWN ON THIS TOPIC

⇒ Recent clinical studies suggest that retinal pigment epithelium (RPE)-cell replacement therapy may preserve vision and restore retinal structure in retinal degenerative diseases. Scaffold-based methods are being tested in ongoing clinical trials for delivering these cells to the back of the eye.

⇒ To investigate the feasibility of the human amniotic membrane (hAM) as a potential scaffold for human embryonic pluripotent cell (hESC)-RPE cells culture.

WHAT THIS STUDY ADDS

⇒ The intrinsic variability of the hAM prevented us from finding an optimal standardisation of the method. In our hands, hESC-RPE cells failed to form a regular monolayer of cells when cultured over the biological tissue.

HOW THIS STUDY MIGHT AFFECT RESEARCH, PRACTICE OR POLICY

⇒ Many aspects should be carefully addressed when intending to use biological tissues in cell therapy applications. First of all, an early selection of the hAM tissue would be preferred prior to any research or clinical use.

INTRODUCTION

Age-related macular degeneration (AMD) is the leading cause of blindness among the elderly in Western countries and affects more than 50 million individuals worldwide.[1]

AMD can be classified broadly into two categories, the non-exudative or so-called 'dry' form and the exudative or 'wet' form. Both types result in photoreceptor degeneration, due to the abnormal alteration of the underlying Bruch's membrane and retinal pigment epithelium (RPE) cells, whose function is irreversibly damaged. Surgical and antiangiogenic treatments are currently available for the wet form of AMD, while there are no approved therapies for the dry form, which accounts for 80–90% of all AMD cases.[2]

In the last decade, cell therapy products designed for RPE cells replacement have been shown to rescue photoreceptors and prevent visual loss in preclinical models of macular degeneration.[3 4] Previous subretinal transplantation with fetal or adult RPE cells has demonstrated limited long-term success.[5–7] Many groups have focused on pluripotent stem cells for their self-renewal potential and ability to differentiate into functional RPE cells capable of restoring visual activity in vivo in Royal College of Surgeons (RCS) rats.[8 9] Current clinical trials are under investigation

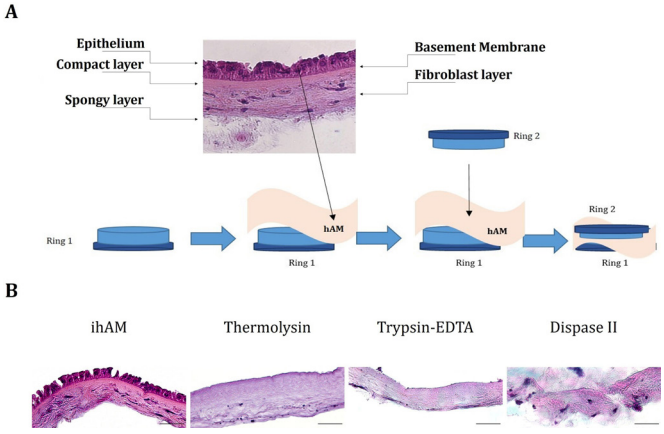

Figure 1 (A) Schematic presentation of the locking of the hAM: the hAM is placed on the Ring 1 of the Amnio Ring with the epithelial layer facing upwards. Ring 2 is placed inside to block it. (B) H&E staining of ihAM (A) and dhAMs after thermolysin (B), trypsin-EDTA (C) and dispase II (D) treatment. Scale bars=50 µm. dhAM, denuded hAM; hAM, human amniotic membrane; ihAM, intact hAM.

to assess the most efficient method to deliver the cell therapy product to the back of the eye.[10–16] A previous study reported a better outcome of RPE cell sheet transplantation over the injection of RPE cell suspension when the same cells were grafted in RCS rats.[17]

The main challenge for the transplantation of an RPE monolayer remains the selection of the scaffold as support for RPE cells. Different materials have been tested and some of them are under investigation in ongoing clinical trials.[10 13 14] The choice of the right matrix is based on required biocompatible properties. To fulfil the need for a permeable, flexible and non-toxic environment for RPE cells, we focused on human amniotic membrane (hAM). The extensive use of this membrane in regenerative ophthalmology is due to its recognised anti-inflammatory and antiangiogenic properties. Besides, it has been demonstrated that it can be integrated successfully into the host tissue after ocular surface reconstruction, helping to renew the structural integrity of the tissue itself.[18 19] A crucial feature of hAM is the close resemblance between its basement membrane (BM) and the Bruch's membrane, which is the native substratum of the RPE cells.

Hitherto, only a few research groups have investigated the fate of donor RPE cells from primary human adult or rabbit RPE over hAM. These studies highlighted the feasibility of the hAM as a support for the growth and differentiation of RPE cells.[20–24]

To date, only one group has reported the culture of human embryonic stem cell (hESC)-derived RPE cells on denuded hAM (dhAM) and their implantation as a designed cell therapy product in the subretinal space of dystrophic rats and non-human primates.[17 25]

Despite these promising results, the handling of the hAM still remains a significant challenge due to its slippery surface and natural tendency to crease and wrinkle.

To enable the exposure of the hAM's BM to promote RPE cells attachment, several de-epithelialisation methods have been proposed. At this stage, complete removal of human amniotic epithelial cells and conservation of the BM itself must be of primary concern.

Herein, we compared different enzymatic de-epithelialisation methods and evaluated their efficacy by appraising the integrity of the hAM and the best cell-seeding outcome. The result of the denudation procedure was assessed by means of optical coherence tomography (OCT), as a new tool to appreciate the quality of non-ocular-related tissues.

In addition, we tested different hESC-derived RPE cells culture conditions over hAM substrate to investigate their functional and molecular properties.

MATERIALS AND METHODS

hAM preparation: enzymatic de-epithelialisation methods

The hAMs were obtained from the Treviso Tissue Bank (Treviso, Italy), with written informed consent from the donor for use in research. Chorion-free tissue samples were preserved at −80°C in cryopreservation medium containing 10% dimethyl sulfoxide and 10% human albumin. The hAMs were thawed at 37°C immediately before use and washed three times with phosphate-buffered saline (PBS). The samples were then locked in an Amnio Ring,[26] with the epithelial side facing up, to prevent the hAMs from slipping or detaching during the treatment (figure 1).

Three different protocols were followed for hAM de-epithelialisation: (1) incubation with 1.2 U/mL dispase II (Sigma-Aldrich, USA) in PBS for 30 min at room temperature (RT); (2) treatment with 0.25% trypsin-EDTA (Life Technologies, USA) in PBS for 30 min at 37°C; and (3) incubation with 3.75 U/mL thermolysin (Sigma-Aldrich, USA) for 9 min at 37°C.[27] The treated hAMs were gently brushed with an absorbent surgical sponge to remove the remaining epithelial cells. The brushing was performed under a stereomicroscope to guarantee a complete removal of the remaining hAM epithelium. Intact hAMs (ihAMs) were retained as controls. We tested five different 10×10 cm pieces of hAM, sourced from six different donors. Each of these 10×10 cm pieces was then cut into 12 smaller pieces, in order to randomly test each denudation method in triplicate on the same donor (plus the untreated control condition).

Optical imaging

To analyse correctly the samples in a vertical position and in a liquid medium, a 6-well flat bottom polystyrene multiwell cell culture plate (Corning, USA) with compatible lid was used. The silicon rings blocking the hAM samples were positioned at the bottom of the wells and then filled with PBS. The wells were sealed with Parafilm (Bemis Company, USA) to prevent leakage. A spectral domain OCT machine was used for this study: the Spectralis retinal OCT adapted with an anterior segment module (Heidelberg Engineering, Germany). Images

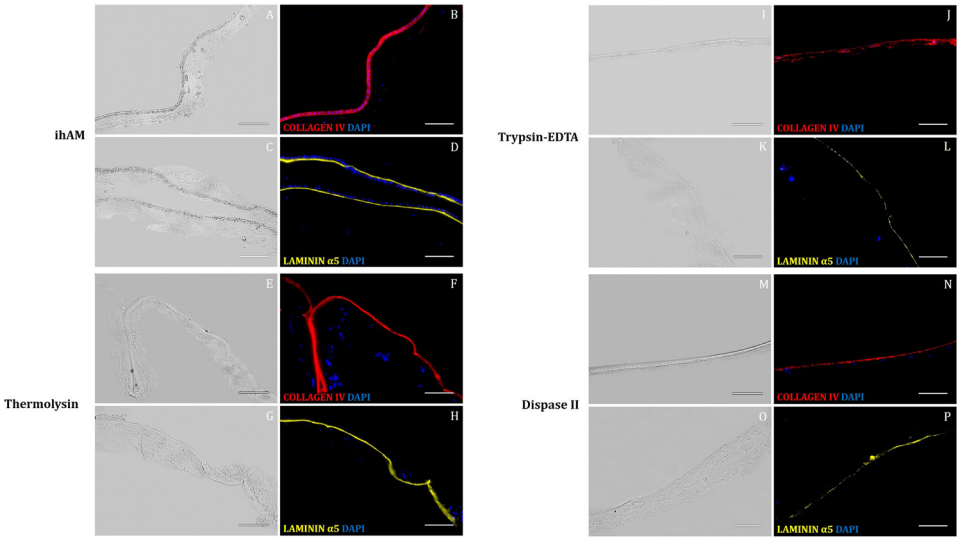

Figure 2 Immunostaining for basement membrane markers, type IV collagen (B, F, J, N; red) and laminin α5 (D, H, L, P; yellow) in cryopreserved ihAM (B, D) and following denuding using thermolysin (F, H), trypsin-EDTA (J, L) and dispase II (N, P). Human amniotic epithelial cell and stromal cell nuclei were stained with DAPI (blue). Scale bars=100 µm. hAM, human amniotic membrane; ihAM, intact hAM.

were analysed with the HEYEX V.6.16.7. All measurements were performed by the same OCT operator (NR), and were collectively evaluated by all the authors.

hESC culture and differentiation toward RPE cells lineage

The hESC line WA09 (WiCell Research Institute, Madison, Wisconsin, USA) was maintained in a feeder-independent culture system on human recombinant laminin-521 (LN-521; BioLamina, Sweden) in Essential 8 Flex Medium (E8; Thermo Fisher Scientific). The genetic profile of the cells was established by the WiCell Research Institute Quality Department (Madison, Wisconsin, USA).

Differentiation into RPE cells was carried out following the protocol outlined by Hongisto *et al*.[28] Briefly, undifferentiated hESCs were single-cell passaged with TrypLE Select Enzyme (Gibco, Thermo Fisher Scientific) and moved to Thermo Scientific Nunclon Sphera Plate, in 15% KnockOut Serum Replacement (KO-SR) medium, consisting of KnockOut Dulbecco's Modified Eagle's Medium (KO-DMEM) containing 15% KO-SR, 2 mM GlutaMAX, 1% MEM Non-Essential Amino Acids, 0.1 mM 2-Mercaptoethanol and 50 U/mL penicillin–streptomycin (all from Gibco, Thermo Fisher Scientific), supplemented with 10 µM Blebbistatin (Sigma-Aldrich), to promote suspension culture through embryoid bodies (EBs) formation.

After 5 days, EBs were transferred to adherent culture and allowed to spontaneously differentiate in 15% KO-SR medium. Three weeks later, pigmented foci with RPE-morphology were mechanically dissected and digested using TrypLE Select Enzyme for ~6 min at 37°C. Isolated RPE cells were plated on LN-521 and collagen IV (CIV; Sigma-Aldrich) coated plates. Sixty days after differentiation started, cells were moved on LN-521+CIV-coated polyethylene terephthalate tissue culture (TC) inserts with 1.0 µm pore size (Sarstedt) until full maturation, which occurred after 12 weeks on the inserts. Derived RPE cells cultured on precoated TC inserts were used as controls. Supplemental information includes schematic diagram of the differentiation process from hESC and details of RPE cells characterisation (online supplemental appendix 1, online supplemental figures A1–A5).

hESC-derived RPE cell culture over hAM

hAMs were locked into the silicon ring and treated with thermolysin enzyme as described earlier. Immobilised hAMs were placed in a 12-well tissue culture plate. The hESC-derived RPE cells from second to third passages were seeded at a density of 2.0×10^5 cells/cm^2 on each locked hAM filled with KO-DMEM supplemented with 10% fetal bovine serum for its adhesion-promoting properties. Medium was changed twice a week. Cultures were maintained for up to 4 weeks. Some hESC-derived RPE cells derived from the same batch were cultured on LN-521+CIV-coated plastic or LN-521+CIV-coated cell culture inserts in 15% KO-SR medium and used as controls.

Histology and immunostaining

Treated and control hAMs were fixed with 4% paraformaldehyde in PBS and left overnight at 4°C, then rinsed three times in PBS. For cryosections, fixed tissue samples were first placed in 7% Sucrose (Sigma-Aldrich, USA), then in 15% Sucrose in PBS for ~4 hours and then stored overnight in 30% sucrose in PBS. The following day, samples were embedded in Cryobloc compound (Diapath, Italy), taking care to avoid bubbles. Cryosections (7 µm thickness) were stained with H&E and visualised using an optical microscope (Zeiss, Germany).

For immunofluorescence, the tissue samples were permeabilised using 0.5% Triton X-100 solution for 30 min. After three PBS washings, they were blocked

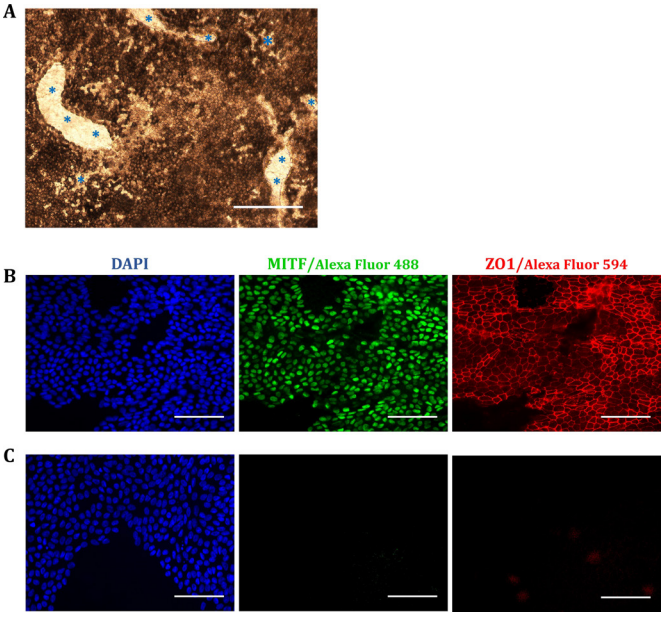

Figure 3 (A) Optical microscope image of hESC-RPE cells on dhAM locked into the amnion ring, 4 weeks post-seeding. Groups of pigmented cobblestone-like RPE cells are scattered across the tissue, among areas of empty dhAM (blue asterisks). Scale bar=100 µm. (B, C) Marker analysis of hESC-RPE cells grown on top of thermolysin-dhAM: positive control staining for MITF (green) and ZO1 (red) (B) and negative control staining (primary antibodies omitted) (C). The nuclei were counterstained with DAPI (blue). All scale bars are 100 µm. dhAM, denuded human amniotic membrane; hESC, human embryonic stem cell; RPE, retinal pigment epithelium.

in 5% bovine serum albumin in PBS for 30 min at RT. Samples were then labelled with mouse anti-MITF monoclonal antibody diluted 1:100 (ab3201, Abcam, UK), rabbit ZO1 polyclonal antibody diluted 1:200 (61–7300, Life Technologies, USA), mouse anti-collagen type IV α2 chain diluted 1:100 (MAB1910, Merck Germany) mouse anti-laminin α5 chain antibody diluted 1:150 (MAB1924, Merck, Germany), rabbit PMEL-17 polyclonal antibody diluted 1:100 (PA5-101023, Life Technologies, USA) and rabbit anti-RPE65 monoclonal antibody, diluted 1:200 (ab231782, Abcam, UK), overnight at 4°C. Rhodamine Red-X goat anti-mouse IgG (1:500; R6393), Alexa Fluor 488 donkey anti-rabbit IgG (1:500; A21206) Alexa Fluor 488 donkey anti-mouse IgG (1:200; A21202) and Alexa Fluor 594 donkey anti-rabbit IgG (1:200; A21207) (all from Life Technologies, USA) were used as secondary antibody for 1 hour at RT. After three PBS washes, the tissues were mounted on glass slides with DAPI Fluoromount-G (Electron Microscopy Sciences, USA) and imaged using the Nikon fluorescent microscope.

PEDF quantification

The hESC-derived RPE cells over hAM and hESC-derived RPE cells cultured on precoated TC inserts (used as controls) were incubated in serum free media for 48 hours. Subsequently, apical and basal media from the Amnio Ring[26] and the precoated TC insert were collected. ELISA was performed to assess the amount of pigment epithelium-derived factor (PEDF) secreted in the RPE conditioned culture medium with the Human SERPIN F1 ELISA kit (Thermo Fisher Scientific) and analysed at 1:2 dilution according to the manufacturer's instructions. The data on PEDF secretion are expressed as mean±SD. Two-way analysis of variance followed by Bonferroni comparisons test was performed using GraphPad Prism V.5.0.0 (GraphPad Software, San Diego, California USA). Values were considered statistically significant at p values<0.05.

RESULTS

Evaluation of hAM de-epithelialisation techniques

Histological examination of the hAM samples showed that all three enzymatic methods (thermolysin, trypsin-EDTA and dispase II) were comparable in terms of hAM de-epithelialisation efficiency, while maintaining the tissue structure. Only a few epithelial cells occasionally remained on dhAM with no differences in trypsin-EDTA and thermolysin treatments. Overall, tissue structure was maintained in both de-epithelialisation methods. On the other hand, we observed severe damage to the hAM architecture and some fragmentation of the stromal matrix following dispase processing (figure 1B).

Intact and thermolysin-treated hAM cryosections showed positive staining for laminin α5 and CIV in the BM, thus indicating a uniform and well-preserved BM in hAM devoid of epithelium. Partial damage to the BM was observed after trypsin-EDTA treatment, with frequent laminin α5 and CIV unlabelled regions interspersed among the BM. Positive staining for laminin α5 and CIV was present in dispase-treated hAM cryosections, but with more diffuse and faint signals than in the ihAM, demonstrating a loss of tissue integrity (figure 2).

OCT analysis of hAM

Spectralis OCT was unable to provide metric measurements due to the HEYEX software requiring a correction of the refractive curvature similar to that of the human cornea, in contrast to the flat surface of multiwell plates. As expected, sample thickness correlated with the degree of tension exerted on the membrane blocked by the rings, for example, a loosely blocked membrane appeared thicker and more susceptible to vibration with positional changes occurring during the analysis of the multiwell plate. We observed that untreated native epithelium was not detectable by OCT analysis, either before or after enzymatic treatment and mechanical scraping. Residual epithelium adjacent to the margin of the rings or cellular debris could be detected as minute low-reflective ribbons and flecks on the epithelial side of the membrane. The BM appeared as a thick highly reflective band, in continuity with the compact layer of the stroma, from which it was virtually indistinguishable, in accordance to the similarities in molecular composition (online supplemental appendix B, online supplemental figure B1). We could

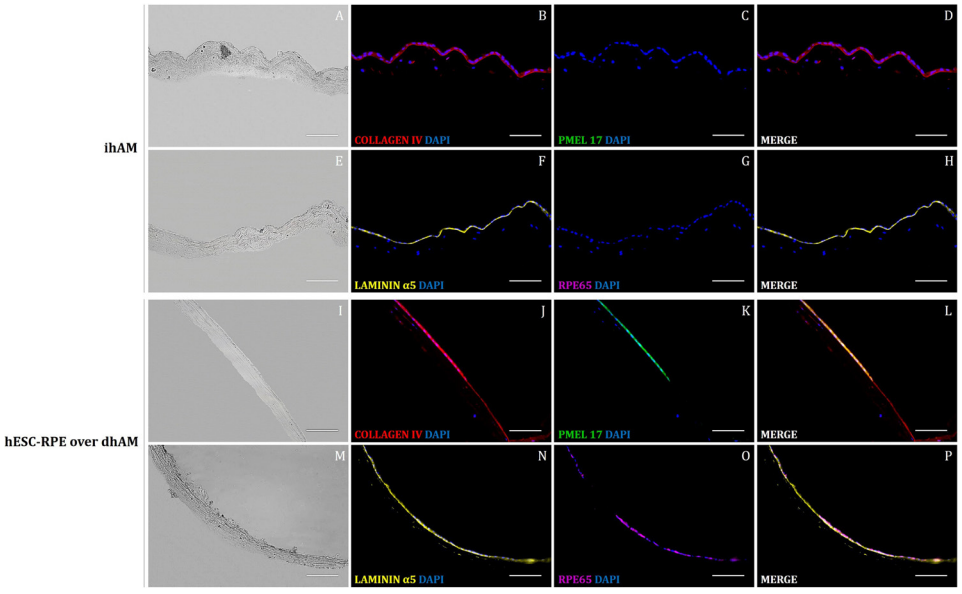

Figure 4 Immunofluorescent staining of RPE differentiation markers, PMEL-17 (C, K; green) and RPE65 (G, O; magenta) and BM markers, type IV collagen (B, J; red) and laminin α5 (F, N; yellow) in cryopreserved ihAM (A–H) and hESC-RPE cells culture on dhAM following thermolysin treatment (I–P). RPE markers identified differentiated hESC-RPE cells over dhAM (K, O), while BM markers demonstrated the preservation of the BM following thermolysin treatment (J, N). Merged images showed areas of membrane where RPE markers were not detected, despite a proper distribution of the BM markers (L, P). ihAM was used as control. hAECs, RPE cells and stromal cells nuclei were stained with DAPI (blue). Scale bars=100 µm. BM, basement membrane; dhAM, denuded hAM; hAM, human amniotic membrane; hESC, human embryonic stem cell; ihAM, intact hAM; RPE, retinal pigment epithelium.

not establish significant differences between the samples that underwent different enzymatic treatments by the means of OCT analysis; any morphological differences, if indeed present, were too minute to be detected by the tomographs at our disposal.

hESC-derived RPE cells culture on thermolysin denuded hAM

The hESC line WA09 was subjected to the spontaneous differentiation method. To achieve a homogeneous monolayer of RPE cells, visible pigmented foci were mechanically isolated and plated in 15% KO-DMEM medium. hESC-derived RPE cells were expanded to passage 2 or 3 and then tested for either characterisation on precoated TC inserts (online supplemental appendix A, online supplemental figures A1–A5) or generation of viable culture over the dhAM. In order to push cell attachment, RPE cells were plated at high density (2.0×10^5 cells/cm^2) in KO-DMEM supplemented with 10% fetal bovine serum on thermolysin pretreated hAM locked into the Amnio Ring.[26] After 4 weeks of hESC-RPE cultured over hAM, patches of pigmented cobblestone-like cells were visible throughout the membrane (figure 3A). These cells showed a positive staining for putative RPE marker MITF, while tight junctions formation was demonstrated by ZO1 staining (figure 3B). Immunofluorescence on cryosections was carried out to assess the BM integrity and generation of an hESC-RPE cells monolayer onto the dhAM. BM markers were found to be strongly expressed in all the samples, forming a bright line, thus showing that laminin α5 and CIV can be clearly detected on the BM (online supplemental appendix C, online supplemental figure C1). Having evaluated the presence of an undamaged BM, we proceeded by identifying hESC-RPE cells using two RPE differentiation markers: PMEL17 and RPE65. Intact hAM was taken as control (figure 4). The consistent expression of PMEL17 and a faint staining for RPE65 further testified the hESC-RPE differentiation on top of the hAM. PMEL17 and RPE65 revealed an irregular staining pattern. Indeed, there were areas of tissue where the two markers were not detected, interspersed between areas of intense or faint expression. These data indicated the lack of a uniform monolayer of cells on top of the hAM, despite the presence of an intact BM (figure 4).

Secretion of PEDF multifunctional protein

Native functionally polarised RPE cells typically secrete growth factors such as PEDF, which provides neurotrophic support to the photoreceptors and serves as angiogenesis inhibitor. PEDF is preferentially released to the apical side of the RPE monolayer. In our experiments, culture supernatants from both the upper and lower chambers of the amnion ring, used to grow the hESC-RPE cells on top of the hAM, were collected after 4 weeks of culture. Conditioned media from hESC-RPE cells cultivated for 4 weeks on precoated TC inserts were taken as controls. We found overall that PEDF was marginally secreted in all the analysed samples (figure 5), compared with other studies conducted on primary RPE cells conditioned media, where PEDF was measured in larger amounts

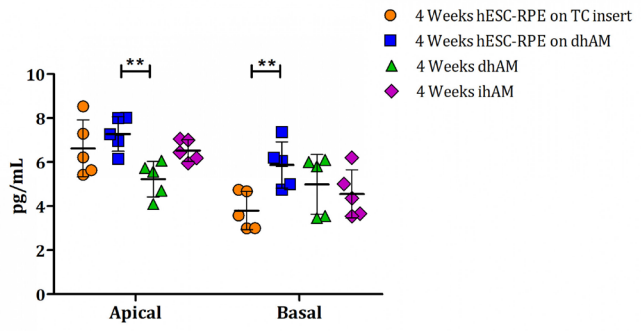

Figure 5 ELISA assay of PEDF secretion by hESC-RPE cells cultured on precoated TC inserts or over dhAM. Concentrations of PEDF in supernatants were normalised to total protein levels of the corresponding collected apical or basal medium volume. The data show an increase of PEDF levels over time only in the apical medium of hESC-RPE cells grown on precoated TC insert. PEDF secretion was detected on both apical and basal media of hESC-RPE cells grown on dhAM with comparable values. PEDF secretion was investigated in apical and basal spent media collected from samples of dhAM without hESC-RPE cells and from samples of ihAM. **p<0.05. Data represent mean±SD of N=5 experiment for each sample. dhAM, denuded hAM; hAM, human amniotic membrane; hESC, human embryonic stem cell; ihAM, intact hAM; PEDF, pigment epithelium-derived factor RPE, retinal pigment epithelium; TC, tissue culture.

(>1 µg/mL).[29] The amount of protein increased with the passage of time of hESC-RPE cells in Transwell cultures, as shown for cells after 8 weeks in culture (online supplemental appendix A, online supplemental figure A5). This suggests that 4 weeks could be an inadequate time for hESC-RPE cultured over hAM for the development of functional polarised cells. Nevertheless, the PEDF level in the apical medium of hESC-RPE cells cultured for 4 weeks on the precoated TC insert was 6.6±1.3 pg/mL (mean±SD, N=5), similar to that in the apical medium of hESC-RPE cells cultured for 4 weeks over hAM (7.3±0.8, N=5) (p>0.05). A significant difference in PEDF levels was found between the apical media of hESC-RPE cells seeded on dhAM and dhAM samples (p<0.05). Interestingly, hESC-RPE cells grown on dhAM showed high levels of PEDF in the basal medium after 4 weeks of culture, compared with low PEDF secretion detected in the basal medium of hESC-RPE cultured on precoated TC inserts for 4 weeks (5.9±1.0 vs 3.2±1.0; p<0.05).

DISCUSSION

In this study, we chose the hAM to act as a supportive biological membrane for culturing hESC-RPE cells.

Human amniotic membrane consists of a single cell layer of epithelium stretched out over a thick BM mainly constituted of type IV collagen and laminin α5, and an avascular stroma composed of interstitial collagen and elastin.[30] Alongside its biocompatibility attributes, the hAM has been well tolerated during experimental surgery in rat retina and shown to stimulate the proliferation of RPE cells in a pig model of choroidal neovascularisation.[31]

With the aim of providing a dynamic microenvironment capable of mimicking the natural structure of Bruch's membrane, our first goal was to identify the most effective process to denude the hAM without damaging the underlying BM. Another important rationale of the de-epithelialisation process was to minimise the immunogenic potential of the hAM in future transplantation experiments, thus decreasing the possibility of a graft failure.[32–34] In addition, the denuding protocol was expected to reduce inter-donor and intra-donor variability among different batches of amniotic membrane,[35 36] and also to increase transparency by lessening the thickness of the tissue. We precluded a whole decellularisation of the hAM samples, in order to preserve important stromal factors critical for cell expansion and wound healing.[37 38] We employed enzyme-based methods to avoid the long treatment time necessary with the use of chemical reagents such as EDTA or SDS.[34 39–41]

The great variability in specimen thickness was determined by the progressive thinning of the hAM the farther the sample was taken from the umbilical cord.[42] OCT evaluation before and after the processing of the hAM allowed us to perform a preliminary morphological assessment of the membrane, evaluating the quality and the thickness of the tissue samples either before or after enzymatic treatment. The paucity of literature on the OCT study of hAM limited the confidence of our findings, especially concerning the results of the enzymatic treatments.[43] Additionally, the software used by the tomographs at our disposal was less than ideal for the task of tissue sample imaging and measuring, given that it had been developed for the in vivo study of cornea and retina.

Laminin α5 and CIV were used to assess the integrity of the hAM's BM. Immunofluorescence staining of the dhAM revealed that all of the three tested de-epithelialisation approaches successfully removed the epithelial cells from hAM surface, but that there was a significant difference between the methods as regards the damage to the BM. In our study, dispase II turned out to be the less safe method for the BM, with a tendency to dissolve several extracellular matrix (ECM) molecules.[44] It also tended to affect the stroma, in line with what had been observed previously by others. In the field of in vivo ocular surface reconstruction, the maintenance of hAM's stromal growth factors seems to be crucial in wound healing and inflammation reduction after hAM transplantation.[45] We speculated that these factors could also be beneficial after the introduction of the hAM into the subretinal space of patients with retinal dystrophy. Incubation with trypsin-EDTA 0.25% kept the BM still mostly intact and maintained stromal integrity. Similar results were obtained with thermolysin, which is a zinc neutral heat-stable metalloproteinase.[46] After thermolysin treatment, we generated a fully dhAM with intact BM and stroma.

Since immunofluorescence alone was not enough to confirm both integrity and eventual minor structural modification of the BM during treatments,[27 30] we set up hESC-derived RPE cell cultures on different pretreated hAMs to highlight any dissimilarities between the cultures. Previous reports on the use of hAM as a biological matrix to sustain RPE growth and differentiation involved primary native RPE cells derived from animal sources or human donors.[20–24] Nevertheless, to our knowledge, there is only one research group working with hESC-RPE cells cultured over dhAM.[17 25 47]

In our hands, hESC-RPE cells seeded over de-epithelialised hAM revealed different outcomes between the performed experiments. We achieved an uneven monolayer of hESC-RPE cells, mainly made of patches of cells scattered along the membrane and interspersed between empty areas of basal membrane. These clusters of cells resembled the typical morphology and pigmentation of RPE cells. The same pattern was observed on cryosections of RPE cells cultured over hAM and stained for RPE 65 and PMEL17. The latter is an integral membrane protein exclusively expressed in pigmented cells and a key component of mammalian melanosome biogenesis. On the other hand, the essential isomerohydrolase RPE65 is involved in the regeneration of the photoreceptor visual pigment during the visual cycle.[48] The expression of the two markers confirmed the formation of a patchy layer of cells on top of the dhAM, with areas devoid of cells. These results showed that in the case the cells adhered and they were able to differentiate properly, they did not form a confluent monolayer. In the aforementioned papers regarding the potential of the hAM to sustain native RPE cells culture,[20–24] the fetal tissue was mostly denuded by enzymatic method, such as 0.25% trypsin and dispase, whereas our study, consistent with more recent findings,[27 44 45] underlined the risk of compromising the BM after the use of such enzymes. Considering the results of the research groups who experimented the culture of native RPE cells over dhAM, we dealt with queer outcomes and incomplete information. Capeáns *et al* showed patches of RPE cells surrounded by areas of bare membrane, demonstrating the attachment of the cells and their organisation in tight colonies of large cuboidal to round cells, but no evidence of a confluent monolayer.[21] In the cases where a monolayer of RPE cells was achieved,[20 22 23] the morphology appears to be seriously jeopardised. Furthermore, the use of native RPE cells could have a significant difference in cell adhesion and proliferation on the dhAM compared with hESC-derived RPE cells. The full in vitro derivation may explain the hardship of these cells to efficiently proliferate over a whole new biological environment, while the isolated primary RPE cells would better recover in a substrate resembling the natural *milieu* of the Bruch's membrane.[24] Future studies on hESC-RPE cells molecular features are needed to validate this latter hypothesis.

It has been proven that cell behaviour on a matrix largely depends on ECM components, that communicate with the cells through cell surface receptors known as integrins, and transmembrane receptors which play an essential role as sensors of the ECM microenvironment.[49] The interaction between ECM proteins and integrins assures cell adhesion and migration over the selected substrate.[50] Based on these considerations, we hypothesised a mismatch between the surface molecules and the corresponding cell receptors.[51] Further tests are needed to establish if this may be linked to a cell deficiency or a partial damage of the BM of dhAM. To invalidate this latter option, a proper electron microscopy examination on thermolysin-treated hAM specimens should be performed, as a way of conclusively confirming BM integrity.[27] The hAM preservation process could also have a negative influence on the culture of hESC-RPE cells over the tissue. Indeed, cryopreservation has been reported to cause severe changes on hAM morphology and biochemical composition.[35] In respect of RPE cells, the use of the same derivation protocol from pluripotent stem cells ensured the manufacturing of high-quality hESC-RPE cells (online supplemental appendix A) and to minimise the variability between different batches of cells. Having tested several of these batches, we concluded that although in some cases the cells were able to adhere, they failed to proliferate on the membrane.

Cultures on dhAM were carried out for a maximum of 4 weeks. After this time, a severe loss of tissue integrity could be appreciated following histological examination. PEDF protein secretion levels were measured for hESC-RPE cells cultured on precoated TC inserts and over hAM for 4 weeks. Comparable levels of PEDF were found between the upper medium of hESC-RPE cells cultivated either on precoated TC inserts or dhAM after 4 weeks. While minimal PEDF secretion was detected in the basal medium of hESC-RPE cells grown on precoated TC inserts, a large amount of PEDF was found in the basal medium of hESC-RPE cells cultured over hAM, equivalent to that one obtained in the apical medium of these samples. These data could lead to different explanations. First, it may suggest a role of the hAM in the production of PEDF. Shao *et al* reported that PEDF is usually expressed in hAM and contributes to the antiangiogenic and anti-inflammatory activities of hAM. In his study, PEDF levels were comparable to those in the human retina, a tissue rich in PEDF.[52] Such findings indicate that PEDF expression after 4 weeks of culture of hESC-RPE cells onto hAM could result from the hAM itself and not from the RPE cells growing onto it. On the other side, the presence of a large PEDF amount in the basal conditioned medium of the hESC-RPE cells cultured over hAM could further prove the lack of a complete RPE cells monolayer on the hAM, since PEDF could soak into cell-free membrane areas.

The biological characteristics of hAM in terms of donor variations have been proven to have a major impact on their physical and chemical properties.[53] The lack of transparency due to the wide variation in the thickness of the membranes supplied made it hard to follow the fate

of the hESC-RPE cells seeded over the tissue. As reported elsewhere, membrane thickness has been correlated with the location in relation to the placenta. OCT imaging evaluation of the thickness could therefore help understanding the distance from the umbilical cord,[42] thus enabling the selection of the best tissue samples with the utmost transparency. Furthermore, the extensive variability of the membranes prevented us from finding a standardised protocol for the handling of the tissue. Age of the donor, as well as gestational age have been shown to affect tissue composition,[36] which may lead to different cell culture outcomes. An early characterisation of the tissue would be preferred prior to any research or clinical use, to select the best tissue to be used as biological substitute to support the host cells.

Ben M'Barek and colleagues demonstrated in their work that the hAM efficiently supports the culture of human pluripotent stem cell-derived RPE cells.[17] However, stressing on the reproducibility limit of the hAM application for the RPE cells, in their results they suggest to check the adhesion of the RPE cells few days after cell seeding. This remark raises the hypothesis of a possible failure in cell attachment as evidence of the variability of the experimental procedure.

This study was limited to a specific biological sample. Our research would benefit from testing RPE cells differentiated from others than hESC WA09 cell lines or multiple WA09 clones. Another potential limitation lies in the inability to conduct additional assays due to hAM thickness. Selecting hAM samples according to thickness might overcome this problem.

In conclusion, although hAM has long been considered an advantageous scaffold in tissue engineering, our results showed that the culture of the WA09 (WiCell Research Institute, Madison, Wisconsin, USA) human embryonic stem cell line-derived RPE cells failed in forming a continuous monolayer over the denuded membrane. Inability of these cells to regenerate a fully functional epithelium onto the support could be due to the previous treatment of the BM. Furthermore, inter-donor and intra-donor factors, as well as hAM processing and storage, should be carefully considered when working on tissue transplantation, where donor selection must be of primary importance.

The lack of standardisation and reproducibility we faced in our work lead us to send up a red-flag to those who intend to use this tissue for cell therapy approaches.

Scaffold-based methods hold great potential in retina tissue engineering, but the development of reliable materials is mandatory. In the field of regenerative medicine, where the candidate therapeutic must comply strictly to Good Manufacturing Practice rules to ensure utmost efficacy and safety, the hAM's path from the bench to the clinic seems to be filled with barriers.

Acknowledgements We gratefully acknowledge Professor Heli Skottman, Dr Tanja Ilmarinen, Dr Heidi Hongisto and biomedical laboratory technicians Outi Melin and Hanna Pekkanen from the BioMediTech Institute, Faculty of Medicine and Life Sciences, University of Tampere, for sharing their expertise on differentiation and characterisation of pluripotent-derived RPE cells and for the critical reading of the manuscript. We thank the staff of the Treviso Tissue Bank (Treviso, Italy) for providing us with the human amniotic membranes used in this study. We are most grateful to Volker Dockhorn from Medicel AG (Altenrhein, Switzerland) for his support and advice in this project and to Gary L A Jones (Veneto Eye Bank Foundation, Italy) as a native English speaker for reviewing the manuscript for clarity.

Contributors ED conceived the idea and supervised the study. ED was responsible for the experimental design. ED, BF and NR conducted experiments, analysed the data and wrote the manuscript. ED, BF, NR and LB conducted experiments. JB-N, VB, SF and DP provided intellectual input. DP is the guarantor of the study. All authors have critically reviewed and edited the manuscript.

Funding This work was partially supported by '5×1000' funds for scientific research from the Italian Ministry of Health and the Italian Ministry of University and Research, and by a Short-Term Scientific Mission grant to ED from the European Cooperation in Science and Technology (EU-COST) Action CA18116 'Aniridia: networking to address an unmet medical, scientific and societal challenge'.

Competing interests None declared.

Patient and public involvement Patients and/or the public were not involved in the design, or conduct, or reporting, or dissemination plans of this research.

Patient consent for publication Not applicable.

Ethics approval Not applicable.

Provenance and peer review Not commissioned; externally peer reviewed.

Data availability statement Data are available upon reasonable request.

ORCID iDs
Elena Daniele http://orcid.org/0000-0001-9900-2767
Stefano Ferrari http://orcid.org/0000-0003-3983-3328

REFERENCES

1 Gehrs KM, Anderson DH, Johnson LV, *et al*. Age-related macular degeneration--emerging pathogenetic and therapeutic concepts. *Ann Med* 2006;38:450–71.
2 Handa JT, Bowes Rickman C, Dick AD, *et al*. A systems biology approach towards understanding and treating non-neovascular age-related macular degeneration. *Nat Commun* 2019;10:3347.
3 Bharti K, Miller SS, Arnheiter H. The new paradigm: retinal pigment epithelium cells generated from embryonic or induced pluripotent stem cells: retinal pigment epithelium cells generated from stem cells. *Pigment Cell Melanoma Res* 2011;24:21–34.
4 Vugler A, Carr A-J, Lawrence J, *et al*. Elucidating the phenomenon of HESC-derived RPE: anatomy of cell genesis, expansion and retinal transplantation. *Exp Neurol* 2008;214:347–61.
5 Blenkinsop TA, Saini JS, Maminishkis A, *et al*. Human adult retinal pigment epithelial stem cell-derived RPE monolayers exhibit key physiological characteristics of native tissue. *Invest Ophthalmol Vis Sci* 2015;56:7085–99.
6 Liu Z, Parikh BH, Tan QSW, *et al*. Surgical transplantation of human RPE stem cell-derived RPE monolayers into non-human primates with immunosuppression. *Stem Cell Reports* 2021;16:237–51.
7 Treumer F, Bunse A, Klatt C, *et al*. Autologous retinal pigment epithelium-choroid sheet transplantation in age related macular

degeneration: morphological and functional results. *Br J Ophthalmol* 2007;91:349–53.
8 Lund RD, Wang S, Klimanskaya I, *et al*. Human embryonic stem cell-derived cells rescue visual function in dystrophic RCS rats. *Cloning Stem Cells* 2006;8:189–99.
9 Thomas BB, Zhu D, Zhang L, *et al*. Survival and functionality of hESC-derived retinal pigment epithelium cells cultured as a monolayer on polymer substrates transplanted in RCS rats. *Invest Ophthalmol Vis Sci* 2016;57:2877–87.
10 Carr A-JF, Smart MJK, Ramsden CM, *et al*. Development of human embryonic stem cell therapies for age-related macular degeneration. *Trends Neurosci* 2013;36:385–95.
11 da Cruz L, Fynes K, Georgiadis O, *et al*. Phase 1 clinical study of an embryonic stem cell-derived retinal pigment epithelium patch in age-related macular degeneration. *Nat Biotechnol* 2018;36:328–37.
12 Kashani AH, Uang J, Mert M, *et al*. Surgical method for implantation of a biosynthetic retinal pigment epithelium monolayer for geographic atrophy: experience from a phase 1/2A study. *Ophthalmol Retina* 2020;4:264–73.
13 Lu B, Zhu D, Hinton D, *et al*. Mesh-supported submicron parylene-C membranes for culturing retinal pigment epithelial cells. *Biomed Microdevices* 2012;14:659–67.
14 Mandai M, Watanabe A, Kurimoto Y, *et al*. Autologous induced stem-cell-derived retinal cells for macular degeneration. *N Engl J Med* 2017;376:1038–46.
15 Schwartz SD, Hubschman J-P, Heilwell G, *et al*. Embryonic stem cell trials for macular degeneration: a preliminary report. *Lancet* 2012;379:713–20.
16 Sharma R, Khristov V, Rising A, *et al*. Clinical-grade stem cell-derived retinal pigment epithelium patch rescues retinal degeneration in rodents and pigs. *Sci Transl Med* 2019;11:eaat5580.
17 Ben M'Barek K, Habeler W, Plancheron A, *et al*. Human ESC-derived retinal epithelial cell sheets potentiate rescue of photoreceptor cell loss in rats with retinal degeneration. *Sci Transl Med* 2017;9:eaai7471.
18 Paolin A, Cogliati E, Trojan D, *et al*. Amniotic membranes in ophthalmology: long term data on transplantation outcomes. *Cell Tissue Bank* 2016;17:51–8.
19 Röck T, Bartz-Schmidt KU, Landenberger J, *et al*. Amniotic membrane transplantation in reconstructive and regenerative ophthalmology. *Ann Transplant* 2018;23:160–5.
20 Akrami H, Soheili Z-S, Sadeghizadeh M, *et al*. Evaluation of RPE65, CRALBP, VEGF, CD68, and tyrosinase gene expression in human retinal pigment epithelial cells cultured on amniotic membrane. *Biochem Genet* 2011;49:313–22.
21 Capeáns C, Piñeiro A, Pardo M, *et al*. Amniotic membrane as support for human retinal pigment epithelium (RPE) cell growth. *Acta Ophthalmol Scand* 2003;81:271–7.
22 Ohno-Matsui K, Ichinose S, Nakahama K-ichi, *et al*. The effects of amniotic membrane on retinal pigment epithelial cell differentiation. *Mol Vis* 2005;11:1–10.
23 Singhal S, Vemuganti GK. Primary adult human retinal pigment epithelial cell cultures on human amniotic membranes. *Indian J Ophthalmol* 2005;53:109–13.
24 Stanzel BV, Espana EM, Grueterich M, *et al*. Amniotic membrane maintains the phenotype of rabbit retinal pigment epithelial cells in culture. *Exp Eye Res* 2005;80:103–12.
25 Ben M'Barek K, Bertin S, Brazhnikova E, *et al*. Clinical-grade production and safe delivery of human ESC derived RPE sheets in primates and rodents. *Biomaterials* 2020;230:119603.
26 Harkin DG, Dunphy SE, Shadforth AMA, *et al*. Mounting of biomaterials for use in ophthalmic cell therapies. *Cell Transplant* 2017;26:1717–32.
27 Hopkinson A, Shanmuganathan VA, Gray T, *et al*. Optimization of amniotic membrane (AM) denuding for tissue engineering. *Tissue Eng Part C Methods* 2008;14:371–81.
28 Hongisto H, Ilmarinen T, Vattulainen M, *et al*. Xeno- and feeder-free differentiation of human pluripotent stem cells to two distinct ocular epithelial cell types using simple modifications of one method. *Stem Cell Res Ther* 2017;8:291.
29 Kanemura H, Go MJ, Nishishita N, *et al*. Pigment epithelium-derived factor secreted from retinal pigment epithelium facilitates apoptotic cell death of iPSC. *Sci Rep* 2013;3:2334.
30 Trosan P, Smeringaiova I, Brejchova K, *et al*. The enzymatic de-epithelialization technique determines denuded amniotic membrane integrity and viability of harvested epithelial cells. *PLoS One* 2018;13:e0194820.
31 Kiilgaard JF, Scherfig E, Prause JU, *et al*. Transplantation of amniotic membrane to the subretinal space in pigs. *Stem Cells Int* 2012;2012:716968.
32 Keane TJ, Swinehart IT, Badylak SF. Methods of tissue decellularization used for preparation of biologic scaffolds and in vivo relevance. *Methods* 2015;84:25–34.
33 Keane TJ, Londono R, Turner NJ, *et al*. Consequences of ineffective decellularization of biologic scaffolds on the host response. *Biomaterials* 2012;33:1771–81.
34 Wilshaw S-P, Kearney JN, Fisher J, *et al*. Production of an acellular amniotic membrane matrix for use in tissue engineering. *Tissue Eng* 2006;12:2117–29.
35 Hopkinson A, McIntosh RS, Tighe PJ, *et al*. Amniotic membrane for ocular surface reconstruction: donor variations and the effect of handling on TGF-beta content. *Invest Ophthalmol Vis Sci* 2006;47:4316–22.
36 López-Valladares MJ, Teresa Rodríguez-Ares M, Touriño R, *et al*. Donor age and gestational age influence on growth factor levels in human amniotic membrane. *Acta Ophthalmol* 2010;88:e211–6.
37 Riau AK, Beuerman RW, Lim LS, *et al*. Preservation, sterilization and de-epithelialization of human amniotic membrane for use in ocular surface reconstruction. *Biomaterials* 2010;31:216–25.
38 Schulze U, Hampel U, Sel S, *et al*. Fresh and cryopreserved amniotic membrane secrete the trefoil factor family peptide 3 that is well known to promote wound healing. *Histochem Cell Biol* 2012;138:243–50.
39 de Melo GB, Gomes JAP, da Glória MA, *et al*. [Morphological assessment of different amniotic membrane epithelial denuding techniques]. *Arq Bras Oftalmol* 2007;70:407–11.
40 Roy R, Haase T, Ma N, *et al*. Decellularized amniotic membrane attenuates postinfarct left ventricular remodeling. *J Surg Res* 2016;200:409–19.
41 Shortt AJ, Secker GA, Rajan MS, *et al*. Ex vivo expansion and transplantation of limbal epithelial stem cells. *Ophthalmology* 2008;115:1989–97.
42 Connon CJ, Doutch J, Chen B, *et al*. The variation in transparency of amniotic membrane used in ocular surface regeneration. *Br J Ophthalmol* 2010;94:1057–61.
43 John S, Kesting MR, Paulitschke P, *et al*. Development of a tissue-engineered skin substitute on a base of human amniotic membrane. *J Tissue Eng* 2019;10:2041731418825378.
44 Lim LS, Riau A, Poh R, *et al*. Effect of dispase denudation on amniotic membrane. *Mol Vis* 2009;15:1962–70.
45 Zhang T, Yam GH-F, Riau AK, *et al*. The effect of amniotic membrane de-epithelialization method on its biological properties and ability to promote limbal epithelial cell culture. *Invest Ophthalmol Vis Sci* 2013;54:3072–81.
46 Miyoshi S, Nakazawa H, Kawata K, *et al*. Characterization of the hemorrhagic reaction caused by Vibrio vulnificus metalloprotease, a member of the thermolysin family. *Infect Immun* 1998;66:4851–5.
47 Ben M'Barek K, Habeler W, Plancheron A, *et al*. Engineering transplantation-suitable retinal pigment epithelium tissue derived from human embryonic stem cells. *J Vis Exp* 2018;139:58216.
48 Weed LS, Mills JA. Strategies for retinal cell generation from human pluripotent stem cells. *Stem Cell Investig* 2017;4:65.
49 Niknejad H, Peirovi H, Jorjani M, *et al*. Properties of the amniotic membrane for potential use in tissue engineering. *Eur Cell Mater* 2008;15:88–99.
50 Mi S, David AL, Chowdhury B, *et al*. Tissue engineering a fetal membrane. *Tissue Eng Part A* 2012;18:373–81.
51 Norde W, Lyklema J. Why proteins prefer interfaces. *J Biomater Sci Polym Ed* 1991;2:183–202.
52 Shao C, Sima J, Zhang SX, *et al*. Suppression of corneal neovascularization by PEDF release from human amniotic membranes. *Invest Ophthalmol Vis Sci* 2004;45:1758–62.
53 Mi S, Chen B, Wright B, *et al*. Ex vivo construction of an artificial ocular surface by combination of corneal limbal epithelial cells and a compressed collagen scaffold containing keratocytes. *Tissue Eng Part A* 2010;16:2091–100.

CHARACTERIZATION OF hESC-RPE CELLS – APPENDIX A

Supplementary methods

Elena Daniele[1,2], Barbara Ferrari[1], Nicolò Rassu[3], Joshua Ben-nun[4], Lorenzo Bosio[1], Vanessa Barbaro[1], Stefano Ferrari[1], Diego Ponzin[1]

1 *Veneto Eye Bank Foundation, Via Paccagnella 11, 30174 Venice, Italy*
2 *University of Ferrara, Via Savonarola 9, 44121 Ferrara, Italy*
3 *Department of Medicine-Ophthalmology, University of Udine, Piazzale S. Maria della Misericordia, 33100 Udine, Italy*
4 *Medicel AG, Dornierstrasse 11, CH-9423 Altenrhein, Switzerland*

PURITY OF hESC-RPE CELLS

Immunohistochemistry and quantitative real-time polymerase chain reaction (Q RT-PCR) were used to confirm the purity of RPE cells culture (Figure A2). Undifferentiated hESC WA09 cell line was taken as positive control. For gene expression analysis, total RNA was extracted with miRNeasy Tissue/Cells Advanced Mini Kit (Qiagen) following manufacturer's instructions and RNA concentration was calculated with Qubit 2.0 Fluorometer (Thermo Fisher Scientific). cDNA was synthesized using the High Capacity cDNA Reverse Transcription Kit (Thermo Fisher Scientific), according to the kit protocol. Q RT-PCR was performed with TaqMan Universal Matermix and predesigned TaqMan assays with FAM-labels (all from Thermo Fisher). The reactions were carried out on ABI Prism 7900HT Sequence Detection System (Applied Biosystems). Relative gene quantification was measured by using the $2^{-\Delta\Delta Ct}$ method. GAPDH was the internal housekeeping gene reference for normalization. Stem cell markers OCT-3/4 and Nanog were not expressed in derived RPE cells, while high expression levels could be detected in hESC WA09 cell line. Immunofluorescence was carried out using the protocol described in the paragraph below.

IMMUNOFLUORESCENCE

hESC WA09 and hESC-RPE cells were washed with PBS and fixed in 4% paraformaldehyde (Santa Cruz Biotechnology) for 15 minutes at room temperature (RT). After several PBS washings, the cells were permeabilized with 0.1% Triton X-100 (Sigma-Aldrich) in PBS for 15 minutes at RT. Cells were washed with PBS and blocked with 3% BSA (Sigma-Aldrich) in PBS at RT for 1 hour to minimize unspecific binding sites. Samples were incubated at 4°C overnight with primary antibodies diluted in 3% BSA at the specified concentrations: Bestrophin 1:100 (PA589606), zonula occludens 1 (ZO-1) 1:200 (61-7300) (both from Thermo Fisher), Na+/K+ ATPase 1:200 (ab7671, Abcam), MERTK 1:50 (H00010461-M01, Abnova), OCT-3/4 1:200 (AF1759) and Nanog 1:150 (AF1997) (both from R&D Systems). The following day cells were washed with PBS and secondary antibodies were added at a dilution of 1:200 in 3% BSA for 1 hour at RT. Alexa Fluor 594-conjugated goat anti-mouse IgG (A11032), 594 donkey anti-rabbit IgG (A21207), 488-conjugated donkey anti-mouse IgG (A21202), A488 goat anti-rabbit IgG (A11034) and 488 donkey anti-goat IgG (A11055) were used as secondary antibodies (all from Thermo Fisher). Nuclei were counterstained with the nuclear dye Hoescht diluted 1:3000 in PBS at RT for 5 minutes. The samples were mounted in ProLong Gold Antifade Mountant without DAPI (Thermo Fisher). Images were captured with Nikon fluorescent microscope (Nikon) using 40x oil immersion objective (Figure A3).

TRANSEPITHELIAL RESISTANCE (TEER)

Transepithelial electrical resistance (TEER) was measured on hESC-RPE cells on TC insert with the Millicell® ERS-2 meter and electrode system (Merck Millipore) at days 28, 35,42,49 and 56 (Figure A4). To obtain true resistance value, resistance measured across the samples was subtracted from resistance read across the controls, respectively denuded hAM and TC insert without cells. Finally, TEER (Ω cm^2) measure was acquired by normalising the resistance value with the surface area of the nitinol ring or the TC insert.

ENZIME-LINKED IMMUNOSORBENT ASSAY

hESC-RPE cell culture supernatants from the upper and lower compartments of the TC inserts were collected after 48 hours of cell culture at 37°C. Harvested media were diluted 1:2 and apical and basal PEDF secretion levels were analysed with Human SERPIN F1 ELISA kit (Thermo Fisher). The remaining media were diluted 1:10 for VEGF quantification using VEGF Human ELISA kit (Thermo Fisher), following manufacturer's instructions (Figure A5). Media volume and insert growth area were used to calculate PEDF and VEGF levels.

FIGURES LEGEND – APPENDIX A

Figure A1: Schematic view with bright-field images of the differentiation process carried out to generate hESC-RPE cells. hESC, human embryonic stem cell; EB, embryoid bodies; RPE, retinal pigment epithelium; LN-521, recombinant laminin-521; CIV, collagen type IV; E8, Essential 8™ Flex Medium; Blebb, blebbistatin; KO-SR, Knock-out™ serum replacement.

Figure A2: Confirmation of a pure culture of RPE cells. (A) Immunofluorescence showing lack of staining for pluripotency associated factors such as OCT-3/4 and Nanog (all green) in hESC derived-RPE cells (upper panel). hESC WA09 cell line was used for comparison (lower panel). Cell nuclei were stained with DAPI (blue). Scale bars = 100µm. (B) Quantitative polymerase chain reaction revealed no expression of OCT-3/4 and Nanog in hESC-RPE. Data are normalized to hESC WA09 cell line. Data represent mean ± SD of N = 3 experiments for each sample. *** $p<0.0001$. hESC, human embryonic stem cell; RPE, retinal pigment epithelium.

Figure A3: Representative immunofluorescence staining indicating the correct expression and localization of typical RPE markers in hESC-RPE cells merged with Heoscht nuclear staining (blue). Scale bars = 100µm. Best1, Bestrophin 1; ZO1, zona occludens-1.

Figure A4: TEER was measured to monitor the barrier function of the hESC-RPE cells on TC inserts over time (days) using a Millicell volt/ohm meter. Data represent mean ± SD of N = 3 experiments for each sample. TEER, transepithelial electrical resistance.

Figure A5: Spent culture media were collected from the apical and the basal chambers of the TC inserts and quantified for PEDF (A) and VEGF (B) concentration using ELISA assays. Data represent mean ± SD of N = 3 experiments for each sample.

Optical Coherence Tomography (OCT) analysis of hAM – APPENDIX B

FIGURE LEGEND – APPENDIX B

Figure B1: OCT evaluation of intact and denuded hAMs. (A) Untreated human amniotic membrane: epithelium, basement membrane and stromal compact layer appear as a thick highly reflective band, and are indistinguishable from each other. A marked distinction can be appreciated between the basement membrane/compact layer and the moderately reflective fibroblast layer. The intermediate spongy layer appears as progressively decreasing in reflectivity starting from the intermediate layer, and it is rich in hypo-reflective spaces and prone to fraying. Denuded hAMs following treatment with (B) dispase II, (C) trypsin-EDTA and (D) thermolysin.

hESC-derived RPE cells culture on thermolysin denuded hAM – APPENDIX C

FIGURE LEGEND – APPENDIX C

Figure C1 Representative immunostaining of BM markers, type IV collagen (B, F, J; red) and laminin α5 (D, H, L; yellow) in cryopreserved ihAM (B, D), denuded hAM using thermolysin (F, H) and hESC-RPE cells culture on denuded hAM following thermolysin treatment (J, L). Dotted rectangles indicate the region that is magnified in the adjacent panels. hAEC and stromal cell nuclei were stained with DAPI (blue). Scale bars = 100 μm. ihAM, intact human amniotic membrane; dhAM, denuded human amniotic membrane, hESC, human embryonic stem cell; RPE, retinal pigment epithelium.

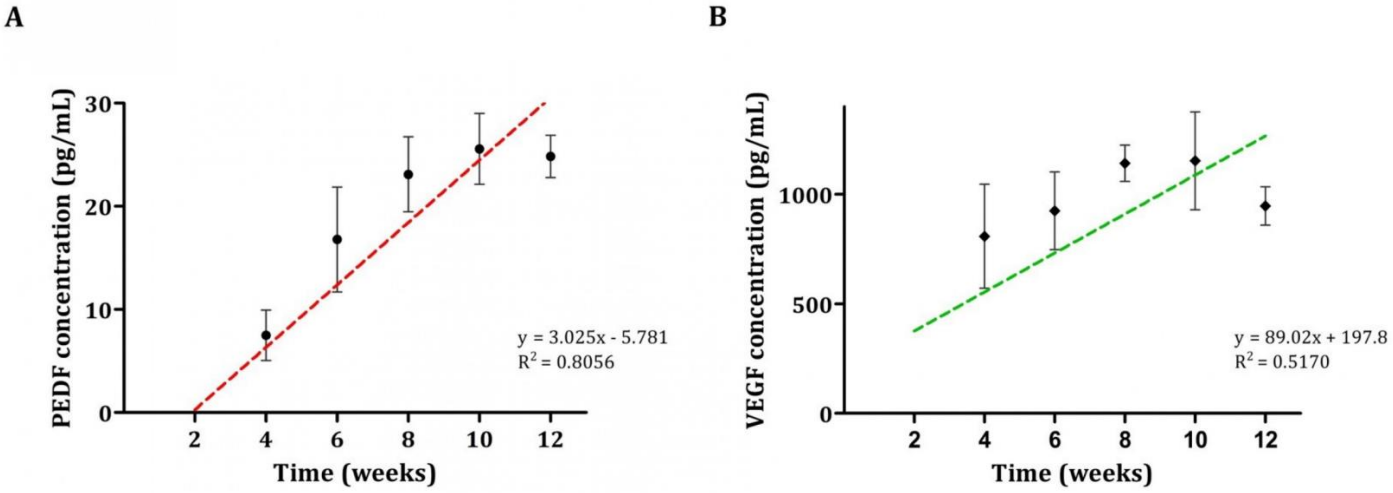
A
PEDF concentration (pg/mL)
30
20
10
0
2
4
6
8
10
12
Time (weeks)
y = 3.025x - 5.781
R2 = 0.8056
B
VEGF concentration (pg/mL)
1000
500
0
2
4
6
8
10
12
Time (weeks)
y = 89.02x + 197.8
R2 = 0.5170

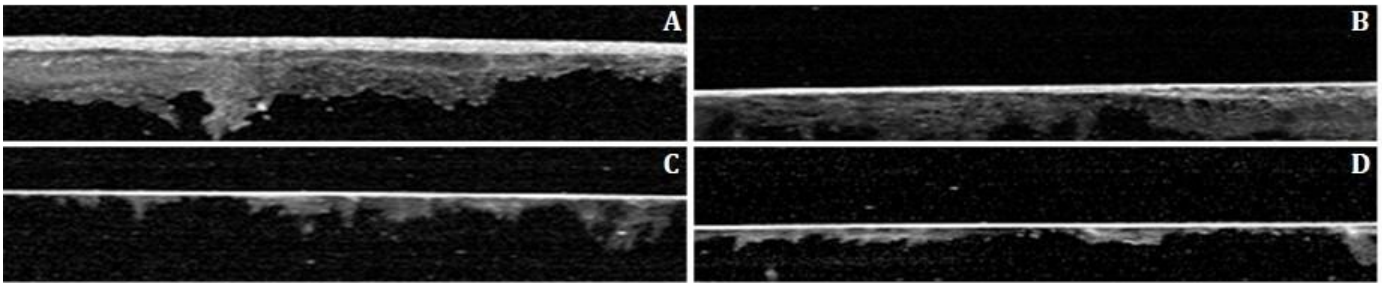
A
B
C
D

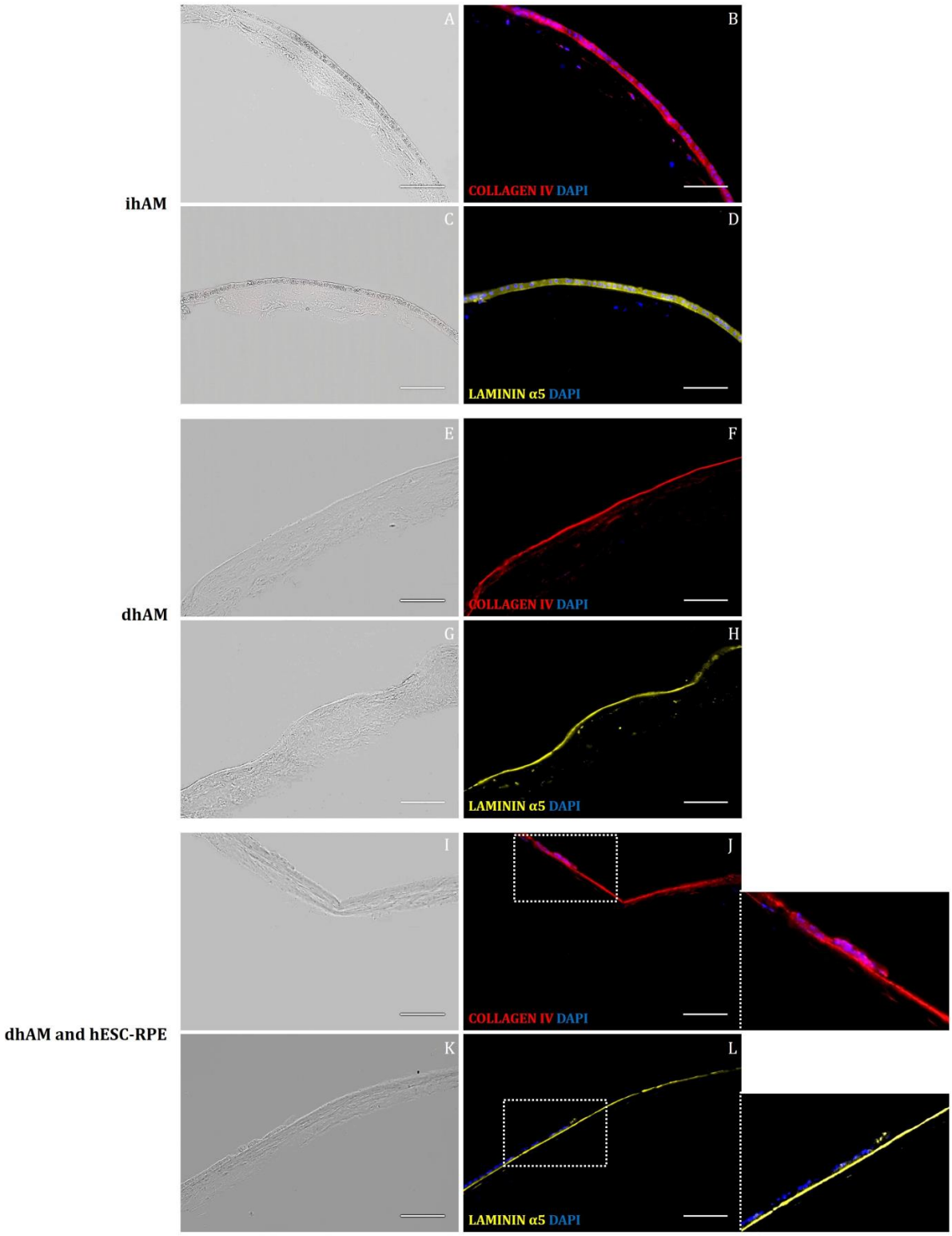
ihAM
dhAM
dhAM and hESC-RPE
A
B
COLLAGEN IV DAPI
C
D
LAMININ α5 DAPI
E
F
COLLAGEN IV DAPI
G
H
LAMININ α5 DAPI
I
J
COLLAGEN IV DAPI
K
L
LAMININ α5 DAPI

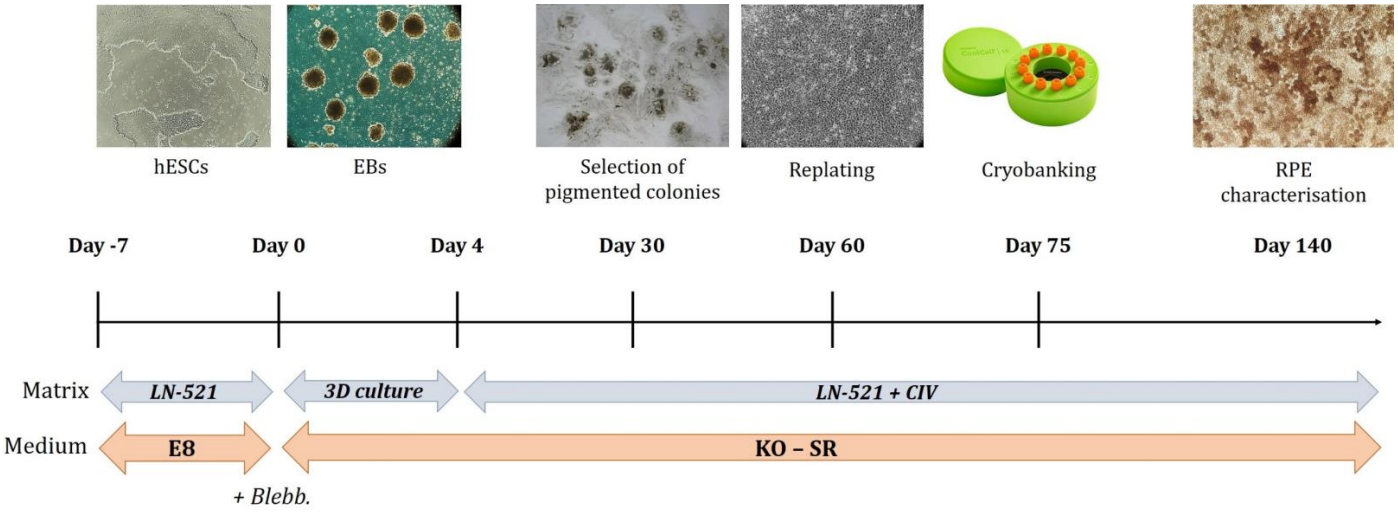
hESCs
EBs
Selection of pigmented colonies
Replating
Cryobanking
RPE characterisation
Day -7
Day 0
Day 4
Day 30
Day 60
Day 75
Day 140
Matrix
LN-521
3D culture
LN-521 + CIV
Medium
E8
KO – SR
+ Blebb.

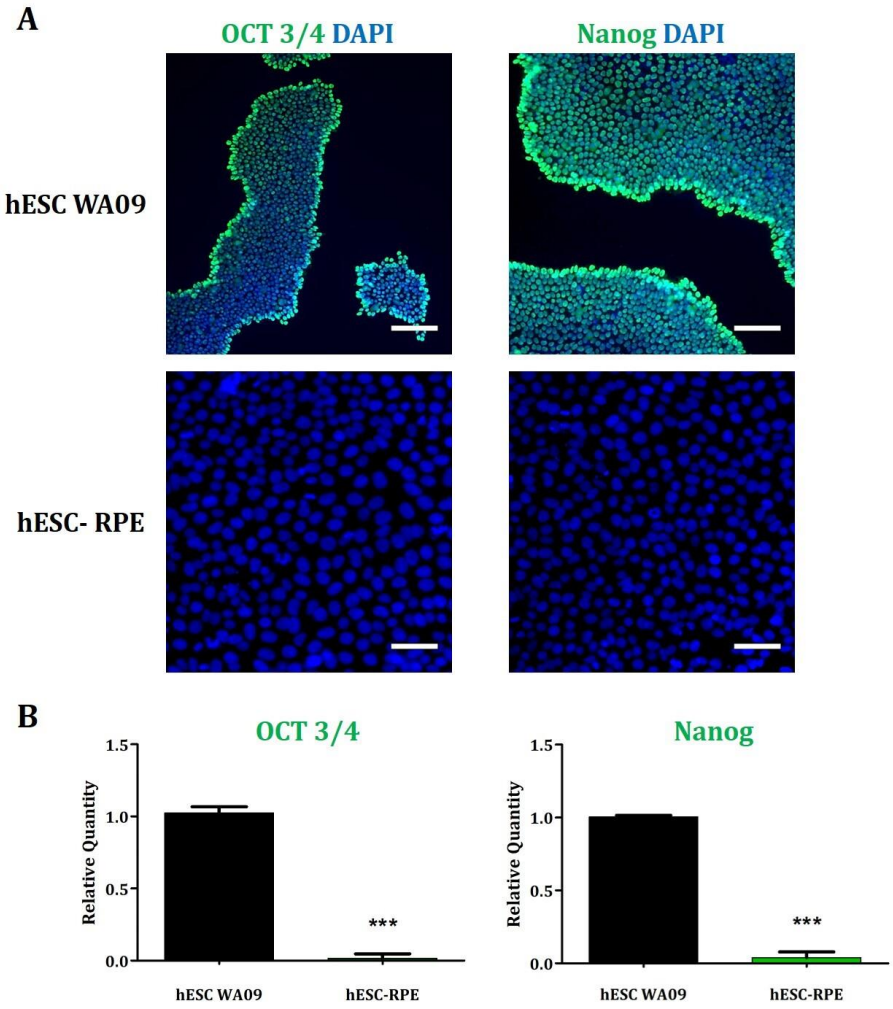
A
OCT 3/4 DAPI
Nanog DAPI
hESC WA09
hESC- RPE
B
OCT 3/4
Nanog
Relative Quantity
1.5
1.0
0.5
0.0
***
hESC WA09
hESC-RPE

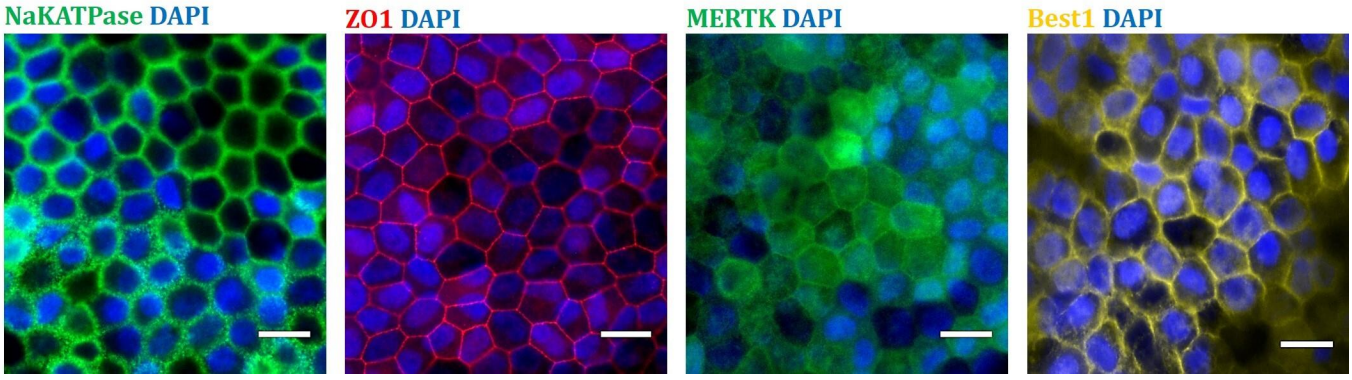
NaKATPase DAPI
ZO1 DAPI
MERTK DAPI
Best1 DAPI

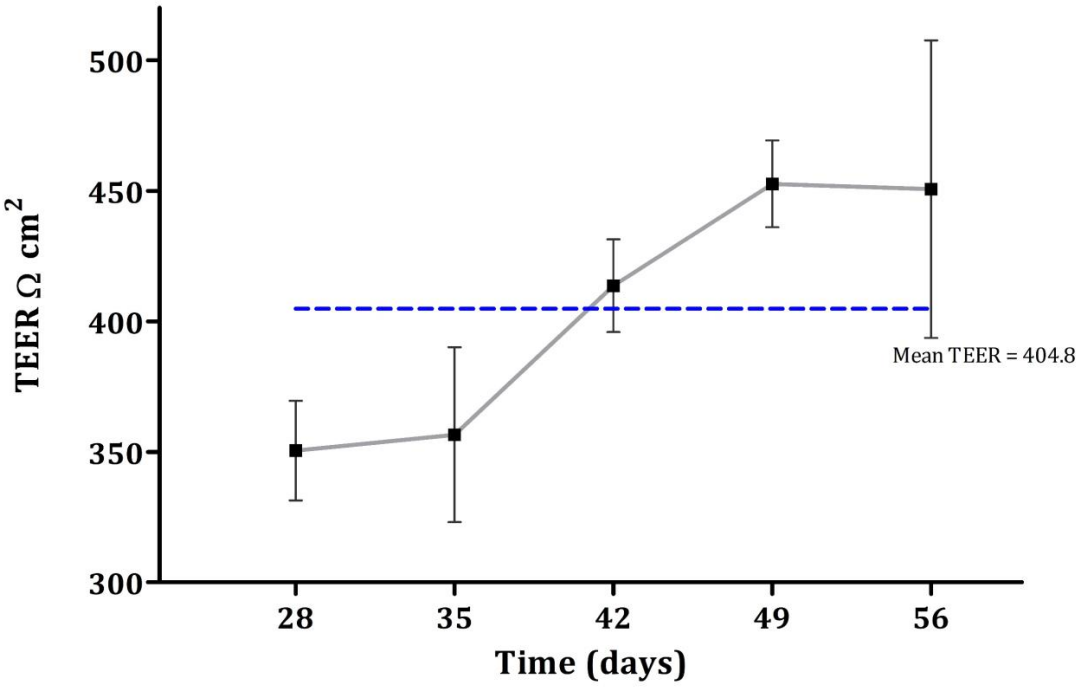
500
450
400
350
300
TEER Ω cm^2
Mean TEER = 404.8
28
35
42
49
56
Time (days)